THE ASTROPHYSICAL JOURNAL, 250:677–686, 1981 November 15

X-RAY EMISSION FROM Of STARS AND OB SUPERGIANTS

J. P. CASSINELLI AND W. L. WALDRON
Washburn Observatory, University of Wisconsin-Madison
W. T. SANDERS
Department of Physics, University of Wisconsin-Madison
AND
F. R. HARNDEN, JR., R. ROSNER, AND G. S. VAIANA[1]
Harvard-Smithsonian Center for Astrophysics
Received 1981 February 2; accepted 1981 May 19

ABSTRACT

The result of a survey of X-ray emission from luminous early-type stars is reported in which observations were made using the imaging proportional counter on the *Einstein* Observatory. The survey suggests that all Of stars and OB supergiants earlier than B1 I are X-ray sources with luminosities $\gtrsim 10^{32}$ ergs s^{-1} and that some later B supergiants have X-ray luminosities $\gtrsim 10^{31}$ ergs s^{-1}. The X-ray fluxes are sufficient to explain the anomalous ionization seen in the ultraviolet spectra of the winds of OB supergiants. The X-ray luminosities are roughly $10^{-7.2}$ of the bolometric luminosities for supergiants earlier than B1 and perhaps a factor of 3 less for later B supergiants. Spectral analysis of the X-rays in conjunction with information on anomalous ionization in the wind from four of the strongest sources implies that the data are not consistent with a model in which the X-rays originate in a thin slab coronal zone at the base of the wind. Constraints on the source of X-rays from B supergiants are derived by combining the X-ray flux information with that on ultraviolet line anomalies. Several models for the source are critically discussed.

Subject headings: stars: Of-type — stars: supergiants — X-rays: sources

I. INTRODUCTION

The winds of early-type stars have been studied primarily through analyses of ultraviolet line profiles and infrared and radio continua (Conti 1978). The studies have not led to a clear picture of the structure of the winds nor of the mechanism by which they are driven. There is sufficient resonance line opacity and momentum flux in the early-type supergiants to drive the high-speed, massive winds (Lucy and Solomon 1970; Castor, Abbott, and Klein 1976; Abbott 1980). However, it has been realized for some time that line-driven wind theories do not adequately account for the anomalously high ionization stages, such as O VI and N V, that are seen with broad P Cygni profiles in the ultraviolet spectra of these stars (Lamers and Snow 1978). Several alternative models which sought to resolve these difficulties have been summarized and discussed by Cassinelli, Castor, and Lamers (1978). One such model, referred to as the "corona plus cool wind model" (Cassinelli and Olson 1979, hereafter CO) suggested that X-rays from a base coronal zone could produce trace amounts of the high ionization stages in the cool wind by the Auger effect, in which two electrons are ejected from an ion following K-shell absorption. This model predicted that Of stars should have an X-ray luminosity of $\sim 10^{32}$ ergs s^{-1} and should be detectable using the imaging X-ray telescope of the *Einstein* Observatory. X-ray emission from early-type stars, at roughly this luminosity, was in fact discovered in the very earliest observations of the *Einstein* Observatory (Harnden *et al.* 1979; Seward *et al.* 1979). Long and White (1980) also reported X-ray emission from hot stars. However, the observed spectra were somewhat softer than predicted in CO, and the suggestion that the hot gas is confined to a thin, hot corona at the very base of the wind was questioned.

This paper presents the results of a more extensive survey of early-type supergiants carried out as part of the *Einstein* Guest Investigator program using the imaging proportional counter (IPC). New observations of 20 optically bright supergiants of spectral type O4f to A2 Ia are presented. We also further discuss the observations of the O4f star ζ Puppis carried out as part of the Columbia University stellar X-ray survey (Long and White 1980). Zeta Puppis has long played a role as a standard object on which tests of stellar wind theories are carried out (e.g., Lamers and Morton 1976). In fact, the corona plus cool wind model of CO was developed using the extensive ultraviolet and optical data available

[1]Also at Osservatorio di Palermo, Italy

for this star. We are grateful to Dr. Knox Long for permission to reanalyze the X-ray pulse-height data from ζ Pup.

The observational data of the 7 O stars and 12 B supergiants, and of the A2 Ia star α Cyg are summarized in § II. Section III presents a more detailed study of the spectra of the four strongest sources. Our aim is to use both the new IPC observations as well as existing information on ultraviolet line anomalies to determine some constraints on the temperature and emission measure of the X-ray source and on the spatial location of the source relative to the wind. Section IV discusses the constraints on coronal sources in the later B supergiants. Conclusions are summarized in § V.

II. OBSERVATIONS

The observations were carried out using the IPC on the *Einstein* Observatory (Giacconi *et al.* 1979). The detection threshold obtained for these observations is about two orders of magnitude fainter than the earlier steller survey of Mewe *et al.* (1975) using *ANS*. The IPC provides source locations to within $\sim 1'$ and pulse-height spectral information with full width at half-maximum resolution $\Delta E/E \approx 1$ at 1.5 keV. The observations were made between 1979 June and 1980 January and consisted of pointings at preselected objects for effective exposure times ranging from 1000 to 7500 s.

The parameters for the stars observed are listed in Table 1 along with data needed in the analysis of the X-ray fluxes: distances to the stars (Abbott 1978; Savage *et al.* 1977; or Humphreys 1978); mass loss rates, $\dot{M}$ (Abbott *et al.* 1980; Barlow and Cohen 1977); terminal wind speeds, v_∞ (Abbott 1978; Cassinelli and Abbott 1981); and interstellar neutral-hydrogen column densities, N_H (ISM) [Bohlin, Savage, and Drake 1978; Humphreys 1978, using $N_H/E(B-V) = 5.8 \times 10^{21}$ cm^{-2} mag^{-1}]. The derived quantities N_w and EM$_w$ are discussed in § III.

For each of the observations of stars of spectral type B0.5 and earlier, except for 29 CMa, a pointlike source of X-rays was detected (at a significance level >5 σ) within $1'$ of the stellar position. (Although 29 CMa, O8.5 If, was not detected in our survey, it was detected as a variable source in the observations of Snow, Cash, and Grady 1981.) Also detected were γ Ara (B1 Ib) and θ Ara (B2 Ib). Although the latter was detected formally at only a 3 σ significance level, a thorough examination of the IPC data indicates that it is an X-ray source. The X-ray data for the observed stars are given in Table 2. Column (1) gives the name of the star and column (2) the effective exposure time. The source counts for most targets were determined from a $6'$ circle centered on the source, and an annulus of inner radius $6'$ and outer radius of $9'$ was used to determine the background. Column (3) gives the net (background subtracted) count rate over the approximate energy interval 0.2–2.5 keV. Indicated uncertainties, based on counting statistics only, for the 10 detected stars are 1 σ. The 3 σ upper limits are given for the stars not detected. The presence of other sources nearby makes the intensity for three stars (9 Sgr, HD 152248, and θ Ara) somewhat more uncertain than the formal errors of Table 2. Systematic uncertainties of

TABLE 1

PARAMETERS OF OBSERVED STARS

Name	Spectral Type	Log T_{eff}	$L_{bol}/10^{39}$ (ergs s^{-1})	R ($R_\odot$)	D (pc)	$\dot{M}$ ($M_\odot$ yr^{-1})	V_∞ (km s^{-1})	Log N_H(ISM) (cm^{-2})	Log N_w (cm^{-2})	Log EM$_w$ (cm^{-3})
9 Sgr	O4f	4.70	4.79	15	1600	2.5−5	3440	21.25	23.44	60.39
ζ Pup	O4f	4.63	3.02	17	430	3.5−6	2660	19.99	22.64	58.85
λ Cep	O6ef	4.57	3.63	24	1000	≤7.8−6	2560	21.40	≤22.86	≤59.43
HD 152248	O8 If	4.50	5.63	40	1900	1.7−5	1700	21.42	23.15	60.24
HD 151804	O8 If	4.48	3.98	40	1800	9.6−6	1710	21.19	22.90	59.74
29 CMa	O8.5 If	4.49	2.51	29	1900	≤6.8−6	1420	20.70	≤22.97	≤59.74
α Cam	O9.5 I	4.46	2.29	32	1200	3.5−6	1890	21.09	22.52	58.87
ε Ori	B0 Ia	4.46	2.29	33	440	3.1−6	2010	20.45	22.43	58.70
κ Ori	B0.5 Ia	4.42	1.44	37	550	≤1.1−6	1870	20.52	≤21.96	≤57.81
γ Ara	B1 Ib	4.32	0.52	30	690	2.3−7	1050	20.71	21.62	57.05
ρ Leo	B1 Iab	4.32	0.63	33	960	1.9−6	1580	20.26	22.32	58.48
139 Tau	B1 Ib	4.32	0.69	35	1200	3.5−7	1500	20.96	21.58	57.04
HD 190603	B1.5 Ia	4.28	1.74	63	1600	≤4.1−6	1300	21.63	≤22.45	≤59.04
χ^2 Ori	B2 Ia	4.26	1.45	63	1380	4.4−7	1100	21.42	21.56	57.25
θ Ara	B2 Ib	4.34	0.63	29	740	3.5−7	1180	20.85	21.43	57.32
55 Cyg	B3 Ia	4.16	0.40	52	1100	1.8−6	830	21.50	22.38	58.80
o^2 CMa	B3 Ia	4.17	0.63	64	1000	3.1−6	600	20.42	22.66	59.46
η CMa	B5 Ia	4.12	0.40	62	760	7.6−7	460	20.42	22.18	58.48
67 Oph	B5 Ib	4.12	0.13	36	760	3.2−7	540	21.14	21.97	57.83
μ Sgr	B8 Ia	4.06	0.91	124	1600	2.4−6	530	21.16	22.32	59.06
α Cyg	A2 Ia	3.96	0.58	156	600	≤2.5−7	280	20.37	≤21.52	≤57.55

TABLE 2

X-RAY DATA OF OBSERVED STARS

Name (1)	Effective Exposure Time (s) (2)	Net Intensity (cts s^{-1}) (3)	F_x (10^{-13} ergs cm^{-2} s^{-1}) (4)	L_x^o (10^{31} ergs s^{-1}) (5)	L_x (10^{31} ergs s^{-1}) (6)
9 Sgr	3906	0.057±0.005	11 ±1	35 ±3	58 ±5
ζ Pup	2529	0.57 ±0.02	114 ±4	25 ±0.9	26 ±1
λ Cep	1827	0.033±0.006	6.5±1.1	7.8 ±1.4	16 ±3
HD 152248	1551	0.037±0.007	7.4±1.4	32 ±6	65 ±12
HD 151804	9698	0.011±0.002	2.1±0.3	8.2 ±1.2	13 ±2
29 CMa	1965	<0.014	<2.9	<12	<14
α Cam	1153	0.027±0.005	5.5±1.0	9.4 ±1.8	13 ±2
ε Ori	1541	0.32 ±0.02	64 ±3	14.8 ±0.7	20 ±1
κ Ori	1757	0.086±0.008	17 ±2	6.2 ±0.6	9 ±1
γ Ara	5705	0.020±0.003	4.0±0.5	2.3 ±0.3	2.7±0.4
ρ Leo	7228	<0.0073	<1.5	<1.6	<1.7
139 Tau	6654	<0.0063	<1.3	<2.2	<2.9
HD 190603	3231	<0.016	<3.3	<10	<28
χ^2 Ori	2734	<0.0047	<0.94	<2.2	<4.4
θ Ara	3013	0.0075 ±0.0022	1.5±0.4	0.98±0.3	1.2±0.4
55 Cyg	7711	<0.0039	<0.79	<1.1	<2.6
o^2 CMa	1770	<0.0074	<1.5	<1.8	<2.0
η CMa	6295	<0.0046	<0.92	<0.64	<0.7
67 Oph	7743	<0.0080	<1.6	<1.1	<1.7
μ Sgr	3138	<0.0091	<1.8	<5.5	<8.5
α Cyg	2879	<0.0056	<1.1	<0.48	<0.5

10–20% dominate for the strong sources. The count rates were converted to X-ray fluxes at the Earth, F_x (col. [4]), using an approximate sensitivity of 2.0×10^{-11} ergs cm^{-2} per IPC count. The flux was converted to an observed X-ray luminosity (col. [5]), $L_x^o=4\pi D^2F_x$, using the distances in Table 1. The value for the L_x^o of ζ Pup differs slightly from that of Long and White (1980) because of a modification in the treatment of the low-energy bins that has been included since the original analysis.

To determine the true X-ray luminosity of the star, which may be of primary interest to stellar structure theorists, L_x^o must be corrected to account for the absorption of X-rays by the interstellar gas and for attenuation by stellar wind material above the X-ray source. Column (6) of Table 2 gives L_x, the X-ray luminosity corrected for interstellar absorption, using N_H (ISM) from Table 1 and a source temperature of 10^7 K (except for ε Ori and κ Ori, for which the fits of § III indicate a temperature $\sim3\times10^6$ K). A crucial aspect of the stellar wind attenuation correction is the location of the X-ray–emitting region(s) within the outer envelope of the stellar atmosphere. X-rays from a source at the base of the wind would be attenuated by the full optical depth of the wind, τ_w, but emission from a source located farther out in the wind would be attenuated by only some fraction of τ_w. The appropriate stellar wind correction factor is therefore very model dependent and has not been applied to the data of Table 2 or Figure 1.

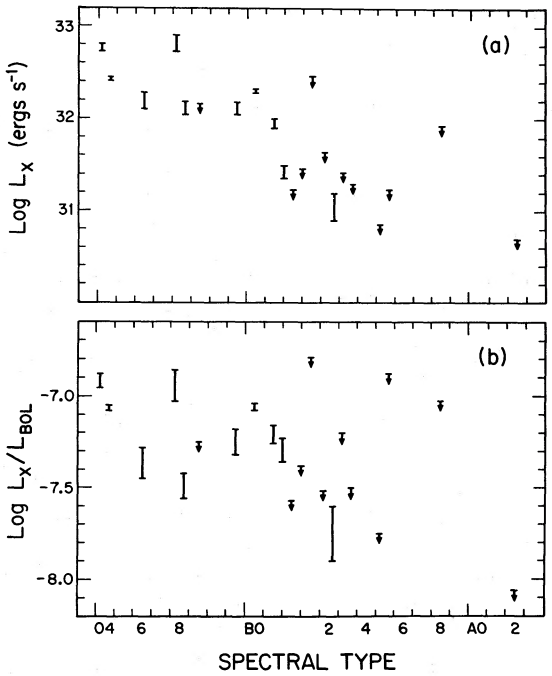

FIG. 1*a*.—The X-ray luminosity corrected for interstellar absorption, L_x, as a function of spectral type for the 21 stars of Table 1. Error bars are ±1 σ. The 3 σ upper limits are indicated by arrows. 1*b*.—The ratio of L_x to the bolometric luminosity versus spectral type.

Figure 1*a* shows the X-ray luminosity corrected for interstellar absorption as a function of stellar spectral type. Previous reports of X-ray observations of early-type stars (of an assortment of luminosity classes) have suggested that L_x is proportional to the bolometric luminosity, L_{bol} (Harnden *et al.* 1979; Seward *et al.* 1979; Long and White 1980). The ratio L_x/L_{bol}, plotted in Figure 1*b* for our sample of supergiants, is very roughly $10^{-7.2}$, but there is a scatter of a factor of 2 about this value. The lack of detections for objects later than B1, except for θ Ara, is consistent with the hypothesis that L_x/L_{bol} is $\leq 10^{-7.2}$ for B and A stars.

III. SPECTRAL ANALYSIS OF THE FOUR STRONGEST SOURCES

A wide variety of possible source models, including wind bubbles and accretion onto compact companions, were discussed by Harnden *et al.* (1979) in the analysis of the X-rays from the early-type stars in the Cyg OB2 association. Because essentially all O stars have X-ray emission, Harnden *et al.* argue strongly for a model in which the X-ray source is intrinsic to the structure of the outer atmospheres of the stars. Furthermore, serious flaws were found with all source models except those in which X-rays are emitted from a hot thermal source embedded in the much cooler stellar wind. Long and White (1980), for their spectral fits, used a model in which emission from an optically thin plasma was attenuated by material with absorption coefficients appropriate to a photoionized wind. As this latter type of model was also used by CO to explain the anomalous ionization in O and B supergiants, we will focus attention on the embedded thermal emission model in our analysis of the strongest four X-ray sources: 9 Sgr (O4f), ζ Pup (O4f), ε Ori (B0 Ia), and κ Ori (B0.5 Ia).

We assume that there is a single region of hot gas at a temperature, T, embedded in the wind under a column density of gas, N_H(WIND). The hot gas is assumed to emit an optically thin emission spectrum (continuum plus lines) as calculated by Raymond and Smith (1979). The monochromatic attenuation of the radiation emitted by the source region depends on the product of the opacity in the intervening regions and the column densities in those regions. For the attenuation by the interstellar gas, we have used the opacity per hydrogen nucleus as given by Brown and Gould (1970). The attenuation by the stellar wind material differs from star to star depending on the ionization conditions in the winds. For very hot stars like 9 Sgr and ζ Pup, there is much less opacity due to singly ionized helium and low stages of ionization of C, N, and O, than there is in interstellar gas or in the winds of the later type stars. As is shown in Figure 2, the opacity at energies less than the carbon K edge at 0.3 keV is much lower for the O4 stars than for the B0 supergiants. We have therefore calculated the

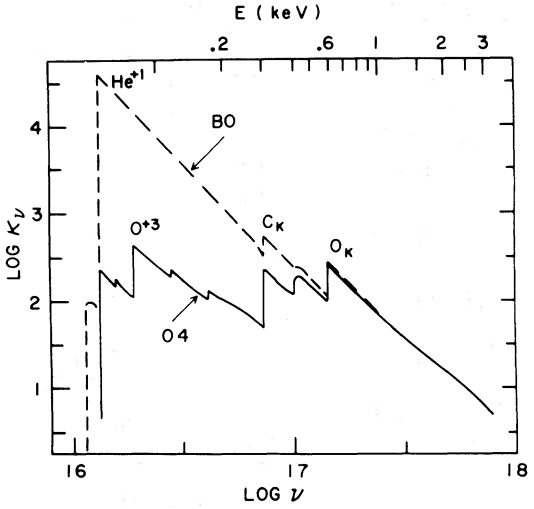

FIG. 2.—Average stellar opacity (cm^2 gm^{-1}) versus frequency (Hz) in the wind of a typical O4f star (*solid line*) and of a B0 supergiant (*dashed line*). The ionization edges of He^{+1}, O^{+3} and the K-shell edges of carbon and oxygen are indicated. These average opacities were calculated by finding the total monochromatic optical depth, as in Cassinelli and Olson (1979), and dividing it by the total mass column density.

stellar wind opacities in detail using the ionization equilibrium program described by CO. The column density of the wind material above a source at radius, R, in the wind is a function of the mass loss rate, $\dot{M}$, and velocity structure:

$$N_H(\text{WIND}) = \int_R^\infty n_H\, dr = \frac{\dot{M}}{4\pi\,\mu m_H} \int_R^\infty \frac{dr}{v(r) r^2}, \quad (1)$$

where v is the velocity and μm_H is the average particle mass.

Given the appropriate wind and interstellar medium (ISM) opacity, the theoretical X-ray spectrum incident upon the detector is determined by the temperature of the source zone, T, by the emission measure of the source region, EM($=n_e^2 V$, where n_e is the electron density and V is the volume of the source region), and by the interstellar and wind column densities, N_H(ISM) and N_H(WIND). For the fits presented here, N_H(ISM) was fixed at the measured value listed in Table 1. For a given set of values of the three remaining free parameters, the IPC pulse-height spectrum was predicted by folding the calculated incident spectrum through the instrumental response. The predicted and observed pulse-height spectra were compared via the χ^2 test and 90% confidence regions were constructed in the manner described by Lampton, Margon and Bowyer (1976). For the strong sources analyzed here, such spectral analysis is limited by the energy resolution and systematic

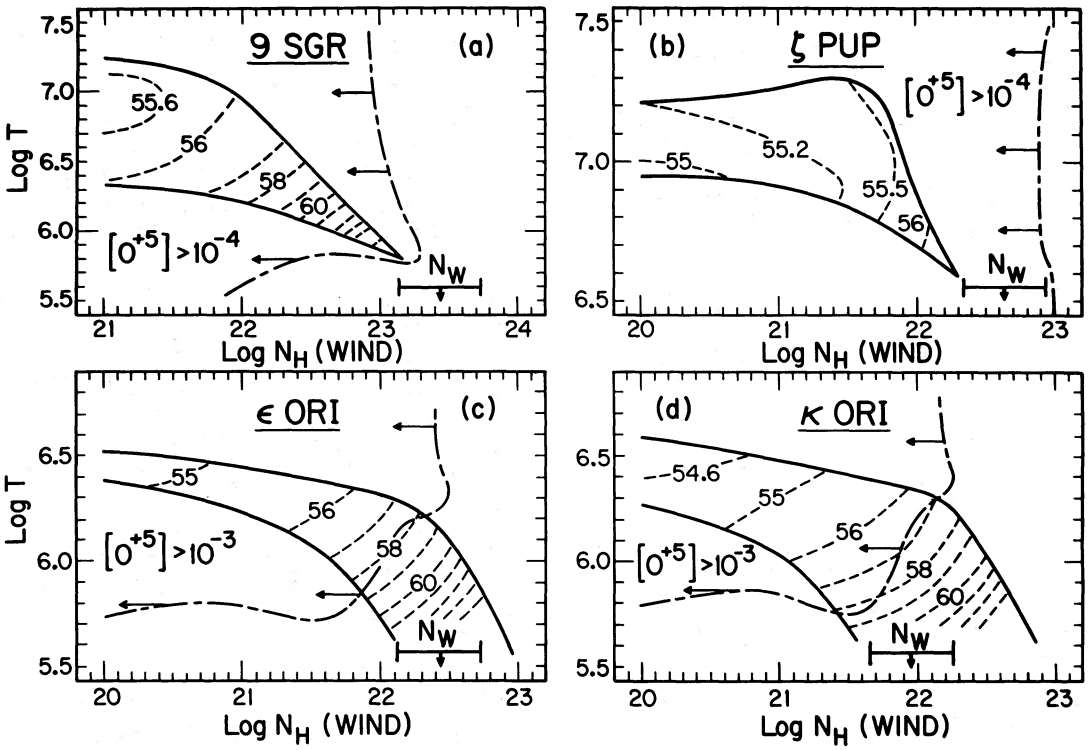

FIG. 3.—The results of the analysis of the IPC spectra of four stars. Between the solid lines are the 90% confidence regions for the temperature and stellar wind column density for the embedded source model. Inside the 90% confidence regions are contours of the logarithm of the best-fit emission measure. In each figure is a dashed line along which the ratio of O VI to O IV has the indicated value. The O VI abundance increases in the direction to the left and above this contour. Also shown is the range of column densities associated with the wind as determined from mass loss rates derived from radio observations.

calibration uncertainties of the IPC. Our calculations allow for the instrumental uncertainties by varying the corrected nominal IPC gain by $\pm 10\%$. Comparison of such calculations with results from independent spectroscopic observations for a variety of stellar X-ray sources has shown this procedure provides very conservative bounds for the derived parameters: T, $N_{\rm H}$(WIND), and EM.

The results of the spectral fittings are shown in Figures 3*a*–3*d*. On a T versus $N_{\rm H}$(WIND) plane are the 90% confidence contours for the two O4f stars and the two Orion supergiants. At each point on the plane in the Figures 3*a*–3*d*, we have specified $N_{\rm H}$(WIND) and the source temperature and have found the minimum χ^2 emission measure of the source. The logarithms of the best-fit EM are shown by the contours inside the 90% confidence regions. We can calculate the X-ray radiation field in the outer regions of the wind to see if sufficient Auger ionization can occur to explain the anomalously strong O VI lines seen in the ultraviolet spectra of these stars. The X-ray enhancement of a high ionization stage can be calculated in an approximate way as described in CO. The O VI lines in O4 stars can be explained if the fractional abundance, O VI/O IV, is as large as 10^{-4} and in B0 stars if it is 10^{-3} (Olson 1978). Contours in the (T, $N_{\rm H}$) plane, where O VI has these abundances, are shown in Figures 3*a*–3*d*. Higher temperatures and/or lower wind column densities would produce more O VI in the outer regions of the wind. Since most of the 90% confidence regions are to the left and above these contours we conclude that O VI is in fact produced in sufficient quantities by the Auger effect independent of the exact parameters of the X-ray emitting region. Long and White (1980) also concluded that the observed soft X-ray flux is sufficient to produce the observed O VI for ζ Pup.

A range of parameter values is consistent with the IPC spectra. At either extreme are (1) high temperatures ($3\text{–}20\times10^6$ K) and low column density, as would be appropriate for coronal zones in the outer regions of a wind, and (2) low temperatures ($0.3\text{–}3\times10^6$ K) and larger column density, as for coronal zones nearer the base of the wind. In the first case, because the radiation is attenuated only weakly by the overlying wind material, the source region is calculated to have relatively small emission measure ($\sim10^{55}$ cm^{-3}). For the second case,

because more of the X-ray radiation is absorbed by the wind, the source is required to have a large emission measure ($>10^{58}$ cm^{-3}). As discussed in CO, a reasonable upper limit for the emission measure of a corona at the base of a stellar wind is the "wind emission measure," EM_w. This is the integral of n_e^2 over the volume of the cool wind, which is assumed to start at the surface of the star, R_*, and have the "standard velocity law" $v(r)^2=v_0^2+v_1^2(1-R_*/r)$ with $v_0=v_1/20$. The quantity EM_w is given by

$$EM_w=2.32\times10^{59}\left(\frac{\dot{M}}{10^{-6}}\right)^2\left(\frac{R_\odot}{R_*}\right)\left(\frac{1000}{v_1}\right)^2 \times \ln\left(\frac{v_\infty}{v_0}\right) \text{ cm}^{-3}, \quad (2)$$

where $\dot{M}$ is here in units of $M_\odot$ yr^{-1} and v_1 is in km s^{-1}. Values for EM_w for the stars in our survey are given in Table 1.

A reasonable upper limit to N_H(WIND) is N_w, the column density to the base of the wind (computed from eq. [1] with $R=R_*$). The value N_w depends on the velocity law and on the mass loss rate. For the velocity law, we have again taken the "standard velocity law" (different velocity laws commonly used in the literature would change N_w by no more than a factor of 2). For the stellar mass loss rates, we have used those deduced from Very Large Array radio observations by Abbott *et al.* (1980). These rates are expected to be especially reliable (Barlow 1979) since they do not depend on knowledge of the temperature or velocity law of the wind. The quantity N_w is given in Table 1 and is shown on Figures 3*a*–3*d*. For κ Ori, the upper limit of the radio mass loss rate and the rate derived from the infrared observations of Barlow and Cohen (1977) bracket 1.0×10^{-6} $M_\odot$ yr^{-1}, and this value is adopted for the calculation of N_w.

There is particular interest in exploring the possibility, discussed in CO, that the X-rays are produced in a slab of coronal material at the base of the wind. In CO, it was assumed that there is a discontinuous drop in temperature between the hot corona and cool wind. This is what we shall call a "slab" corona. This model gives the maximum column density of cool absorbing material between the corona and the observer. The parameters for this slab coronal model must satisfy two additional criteria: (1) N_H(WIND)$=N_w$ and (2) EM$\leq EM_w$. For the four stars of Figure 3, Figure 4 shows the measured IPC pulse-height distributions (with 1 σ error bars) for the best-fit embedded source model and the best-fit slab coronal model. The parameters for these fits are listed in Table 3. The slab coronal model fit for κ Ori is acceptable, but for the other three stars it is very poor. The reason for the poor fits is straightforward. The N_w value is very large. If N_H(WIND)$=N_w$, a rather low value of T is required if the model is to match the shape of the observed pulse-height distribution, and a very large value of the EM (larger than EM_w) is required to reproduce the measured intensity. In reducing the EM to be $\leq EM_w$, T must be raised to minimize χ^2. Even though the best-fit T for the slab corona model is less than the best-fit T for the general embedded source model, the peak of the predicted pulse-height distribution is at higher energies because of the heavy low-energy absorption of the large N_w.

We can conclude from the spectral analysis that: (1) for κ Ori, the source of the observed X-rays could be either a base coronal zone or an exterior coronal zone, but (2) for 9 Sgr, ζ Pup, and ε Ori, the observed X-ray spectrum is not consistent with a source at the base of the wind if the emission measure is constrained to be $\leq EM_w$. (Long and White 1980 reached a similar conclusion in their analysis of the ζ Pup data.) For these three stars, the source must be substantially outside most of the stellar wind material. Three possibilities are that the hot material is distributed throughout the wind (Lucy and White 1980), or that the coronal zone at the base is separated geometrically from the wind (Rosner and Vaiana 1980), or that the coronal zone is more extended than assumed in the slab coronal model (Waldron 1980). These are discussed further in § V.

IV. CONSTRAINTS ON THE CORONAL SOURCES IN THE B SUPERGIANTS

The ionization anomalies in the ultraviolet spectra of luminous early-type stars are seen not only in the O stars but persist well into the B supergiant spectral ranges. The N V (λ1240) line is seen in stars as late as B2.5 I and the C IV (λ1450) line as late as B6 Ia (Cassinelli and Abbott 1981). It is reasonable to assume that these anomalies are also due to the Auger effect caused by X-rays in the winds. The X-ray luminosities of the B supergiants are relatively low, as is seen in Figure 1, but the combination of these X-ray fluxes and the Auger ionization can be used to place constraints on the X-ray sources in these stars. As discussed in § III, given the temperature, emission measure, and attenuation column density, the emergent X-ray luminosity and relative abundance of an anomalous ionization stage in the outer regions of the wind can be calculated (CO). The mass loss rates of several of our B supergiants are known from the free-free emission at infrared wavelengths measured by Barlow and Cohen (1977) and are given in Table 1. From these, we can determine the column density to the base of the wind. From the line strength studies of Olson (1978) and Olson and Castor (1981), we can assume that the anomalously strong lines of N V and C IV require that the relative abundance of these ions be above $\sim10^{-3}$.

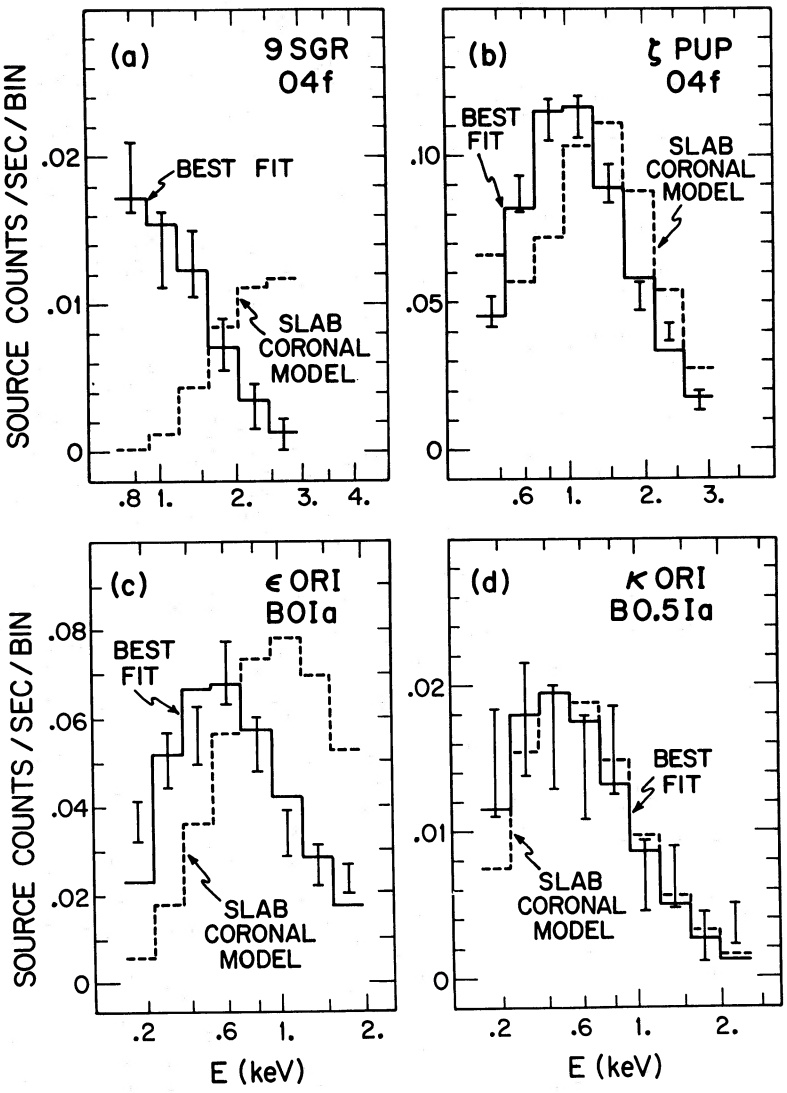

FIG. 4.—The IPC pulse-height spectra in net counts per second per bin versus energy in keV. Also shown are two theoretical fits to the spectra. The solid lines show the best embedded source model and the dashed lines show the results for the best-fit slab corona model. The parameters of these fits are listed in Table 3.

TABLE 3

MINIMUM χ^2 BEST-FIT PARAMETERS FOR TWO MODELS

	BINS	ENERGY RANGE	DEGREES OF	BEST-FIT EMBEDDED SOURCE MODEL				BEST-FIT SLAB CORONAL MODEL			
STAR	FIT	(keV)	FREEDOM	χ^2_{min}	Log T	Log N_H	Log EM	χ^2_{min}	Log T	Log N_H	Log EM
9 Sgr	3–8	0.6–2.7	3	1.0	6.1	22.60	60.98	396	6.6	23.44	60.52
ζ Pup	1–8	0.2–3.0	5	4.8	7.1	21.40	55.27	154	6.4	22.64	58.43
ε Ori	1–8	0.2–2.0	5	17.7	6.1	22.40	59.33	281	6.3	22.43	58.44
κ Ori	1–9	0.2–2.3	6	7.0	6.3	20.70	54.83	12.5	6.2	21.92	56.53

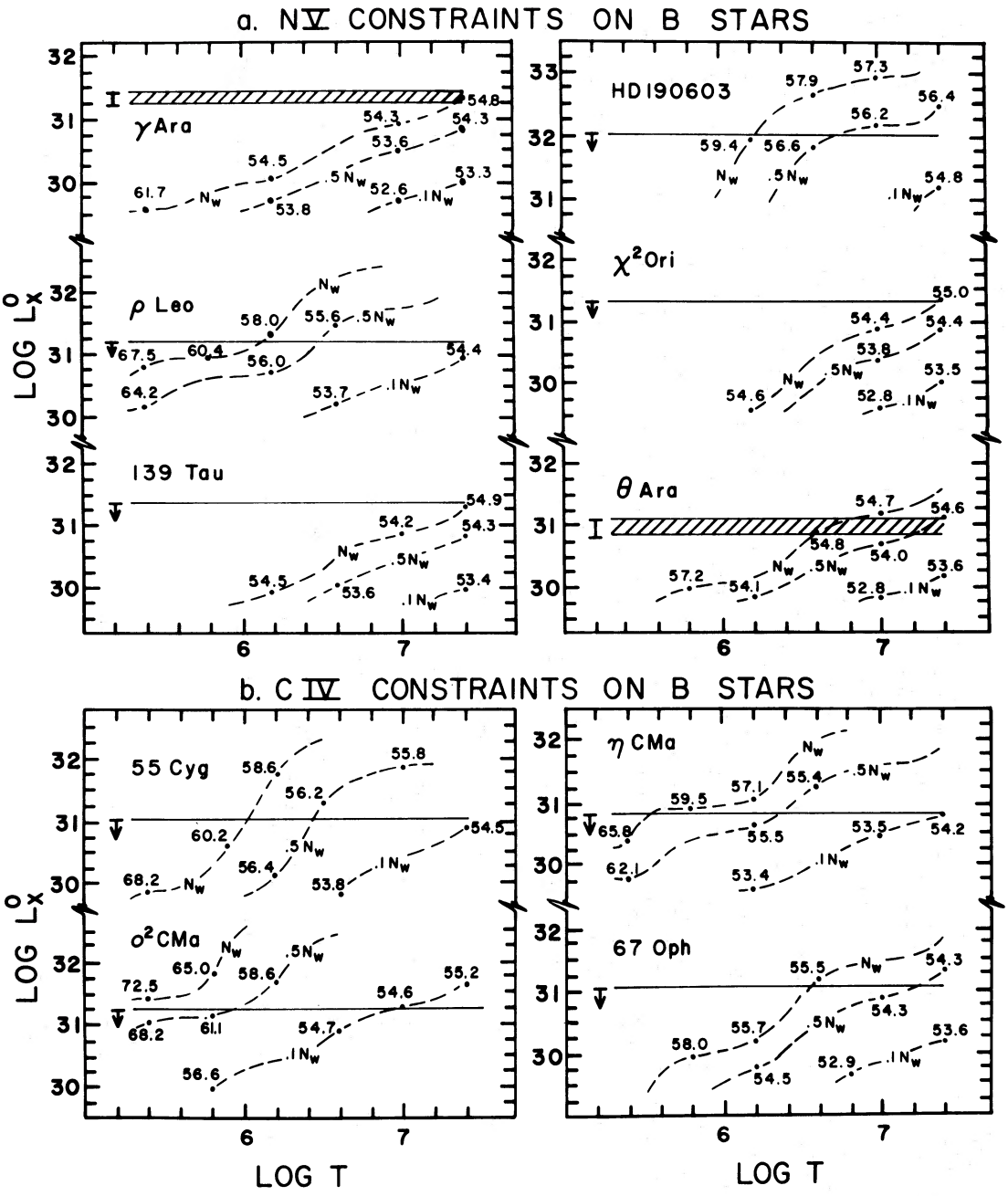

FIG. 5.—Shows several constraints that can be placed on the source of X-rays in the B supergiants from the requirements that (*a*) the abundance ratio N V/N III $\geq 10^{-3}$ in the winds of early B supergiants and (*b*) the abundance ratio of C IV/C II $\geq 10^{-3}$ in the winds of later B supergiants. The observed X-ray luminosity for the detected stars is shown by the shaded region, and upper limits on the luminosity are indicated by the arrows for the other stars. The contours show the theoretical observed X-ray luminosity, L_x^o, for sources of a given temperature, T, at the column density indicated on each contour (e.g., $0.5N_w = 0.5$ of the hydrogen column density to the base of wind). Along each contour are several values for log (emission measure). For several stars, the slab coronal model is seen to require unacceptably large emission measures.

In Figure 5, we show the observed X-ray luminosities as cross-hatched regions and the upper limits as horizontal lines. For Figure 5*a*, the constraint, N V/N III = 10^{-3}, was used for the B supergiants of spectral types B1 and B2, and for Figure 5*b*, the constraint, C IV/C II = 10^{-3} was used for spectral types B3 through B6. Using these constraints, theoretical contours were calculated that give the X-ray luminosity and emission measure as a function of coronal temperature using three values of the hydrogen wind column density: N_w, 0.5 N_w, and 0.1 N_w. These three values correspond to coronal gas at three distinct regions in the flow: (1) for $N_{\rm H}({\rm WIND}) = N_w$, the X-rays are attenuated by the full wind column density as in the slab corona case; (2) for $N_{\rm H}({\rm WIND}) = 0.5N_w$, the attenuation corresponds to a coronal zone in the accelerating region where the velocity is roughly $\frac{1}{2}\ v_\infty$ midway in the flow; and (3) for $N_{\rm H}({\rm WIND}) = 0.1N_w$, the attenuation is for an X-ray–emitting region that is occurring farther out in the flow where the velocity has nearly reached terminal velocity. The contours shown in Figure 5 show the lower limits to L_x^o and EM, as a function of T, necessary to produce enough N V or C IV to be detected. If, instead of a relative abundance ratio of 10^{-3}, we had used 10^{-2}, then each N_w contour would rise along the L_x^o axis by a factor of 10 and the values of the emission measures along the contour would increase by a factor of 10 because EM is proportional to the relative abundance ratio and L_x^o is proportional to EM.

In Figure 5*a*, notice that, for the two detected stars, γ Ara and θ Ara, the slab coronal model is allowed because acceptably small emission measures (e.g., $<{\rm EM}_w$) can explain both the observed X-ray flux and the observed ionization anomaly. A constraint on a coronal temperature can be read off the figure ($T \lesssim 10^7$ K). For ρ Leo and HD 190603, the slab coronal model is not acceptable because of the large emission measure required to produce sufficient N V; ${\rm EM} > {\rm EM}_w$. The source models attenuated by either $0.5N_w$ or $0.1N_w$ are acceptable.

In Figure 5*b*, we see that, for all of these stars except 67 Oph, the slab coronal model can be ruled out as a source of the X-radiation required to produce C IV by the Auger mechanism. For these stars, the source cannot be attenuated by the total column density of the wind. In particular, the results of o^2 CMa imply that even the 0.5 N_w model is unacceptable.

V. DISCUSSION

The IPC spectral data and the information on the ionization anomalies in winds have been used to derive constraints on embedded source models. The analysis has indicated that the source cannot be solely in the form of a thin slab corona at the base of the wind as had been suggested by Cassinelli, Olson, and Stalio (1978) and by CO. The observed X-rays do not appear to be so strongly attenuated as the slab model would suggest. Also, for several stars, the model would require the corona to have an excessively large emission measure in order to explain the presence of ionization anomalies such as O VI, N V, and C IV in the outer reaches of the winds. The X-ray data can be explained by a single coronal region, far out in the flow, with a relatively small emission measure ($\sim 10^{55}$ cm^{-3}). However, because of the small emission measure, this model would have difficulties explaining the ultraviolet line profiles that indicate ionization anomalies exist deep in the flow (at $v \ll v_\infty$). This is because of the large attenuation that would be present in the inward direction.

Three alternative models have been suggested to explain both the observed X-ray data and the ionization anomalies. These require that the hot material either be distributed throughout the wind or be in a base corona which has less overlying attenuation because of the temperature or geometrical structure of the wind.

1. Several studies have found that line-driven winds are unstable (Nelson and Hearn 1978; MacGregor, Hartmann, and Raymond 1979; Martens 1979; Carlberg 1980). In an early explanation of the O VI anomaly, Natta *et al.* (1975) proposed that instabilities produce hot filaments throughout the winds. Lucy and White (1980) have proposed that the instabilities grow to massive blobs that develop hot bow shocks on being driven through the stellar wind. These instabilities and bow shocks would presumably develop in any mechanically quiet star that has a line-driven wind. The shocks distribute, throughout the wind, hot material whose X-ray emission is subject to much less attenuation than that of a slab corona. However, some doubt has been cast on the instability mechanism by which the X-rays are produced. Using the same method as previous authors, but a different expression for the line radiation force, Abbott (1980) does not find instabilities in line-driven winds. More work is clearly needed to resolve this issue.

2. Waldron (1980) has considered the structure at the top of a base corona where, in a recombination region, the flow makes a transition from a corona-driven to a radiatively driven wind. He found that the temperature decrease is not as steep as assumed in the slab coronal model but extends out several tenths of a stellar radius. This leads to a lower opacity which reduces the X-ray attenuation and results in a large increase in the emergent flux of soft X-rays.

3. Rosner and Vaiana (1980) have suggested that the wind outflow covers only a portion of the stellar surface, leaving X-ray–emitting plasma exposed over the remainder of the stellar surface. In this picture, the hot gas would be magnetically excluded from the regions of

greatest mass outflow. This spatial separation would reduce the net attenuation of the outer wind material. One might expect, on the basis of this picture, to see variability in the X-ray flux.

We conclude that the slab model can be ruled out and that detailed spectroscopic and variability studies along with improved measurements of mass loss rates are required to test the remaining models. Improved calculations of the anomalous line profiles for each of the above three cases would also be of value.

We thank Dr. Knox Long for providing us with unpublished spectral data on ζ Pup and Dr. David Abbott for helpful comments. This research was supported in part by NASA grants NAG 8345 and NGL 50-002-004.

REFERENCES

Abbott, D. C. 1978, *Ap. J.*, **225**, 893.
_____. 1980, *Ap. J.*, **242**, 1183.
Abbott, D. C., Bieging, J. H., Churchwell, E., and Cassinelli, J. P. 1980, *Ap. J.*, **238**, 196.
Barlow, M. J. 1979, in *IAU Symposium 83, Mass Loss and Evolution of O-Type Stars*, ed. P. S. Conti and C. W. H. de Loore (Dordrecht: Reidel), p. 119.
Barlow, J. H., and Cohen, M. 1977, *Ap. J.*, **213**, 737.
Bohlin, R. C., Savage, B. D., and Drake, J. F. 1978, *Ap. J.*, **224**, 132.
Brown, R. L., and Gould, R. J. 1970, *Phys. Rev. D*, **1**, 2252.
Carlberg, R. G. 1980, *Ap. J.*, **241**, 1131.
Cassinelli, J. P., and Abbott, D. C. 1981, in *The Universe at Ultraviolet Wavelengths: The First Two Years of IUE*, ed. R. D. Chapman, NASA Conference Pub. 2171, p. 127.
Cassinelli, J. P., Castor, J. I., and Lamers, H. J. G. L. M. 1978, *Pub. A.S.P.*, **90**, 496.
Cassinelli, J. P., and Olson, G. L., 1979, *Ap. J.*, **229**, 304 (CO).
Cassinelli, J. P., and Olson, G. L., and Stalio, R. 1978, *Ap. J.*, **220**, 573.
Castor, J. I., Abbott, D. C., and Klein, R. I. 1976, in *Physique des Mouvements dans les Atmospheres Stellaires*, ed. R. Cayrel and M. Steinberg (Paris: C.N.R.S.).
Conti, P. S. 1978, *Ann. Rev. Astr. Ap.*, **16**, 371.
Giacconi, R., *et al.* 1979, *Ap. J.*, **230**, 540.
Harnden, F. R., *et al.* 1979, *Ap. J.* (*Letters*), **234**, L51.
Humphreys, R. M. 1978, *Ap. J. Suppl*, **38**, 309.
Lamers, H. J. K. L. M., and Morton, D. C. 1976, *Ap. J. Suppl.*, **32**, 715.
Lamers, H. J. K. L. M., and Snow, T. P. 1978, *Ap. J.*, **219**, 504.
Lampton, M., Margon, B., and Bowyer, S. 1976, *Ap. J.*, **208**, 177.
Long, K. S., and White, R. L. 1980, *Ap. J.* (*Letters*), **239**, L65.
Lucy, L. B., and Solomon, P. M. 1970, *Ap. J.*, **159**, 879.
Lucy, L. B., and White, R. 1980, *Ap. J.*, **241**, 300.
MacGregor, K. B., Hartmann, L., and Raymond, J. C. 1979, *Ap. J.*, **231**, 514.
Martens, P. C. H. 1979, *Astr. Ap.*, **75**, L7.
Mewe, R., Heise, J., Gronenschild, E. H. B. M., Brinkman, A. C., Schrijver, J., and den Boggende, A. J. F. 1975, *Ap. J.* (*Letters*), **202**, L67.
Natta, A., Priete-Martinez, A., Panagin, N., and Macchetto, F. 1975, *Laboratorio di Astrofisica Spaziole, Frascati Rapporto No. 23.*
Nelson, G., and Hearn, A. G. 1978, *Astr. Ap.*, **65**, 223.
Olson, G. L. 1978, *Ap. J.*, **226**, 124.
Olson, G. L., and Castor, J. I. 1981, *Ap. J.*, **244**, 179.
Raymond, J. C., and Smith, B. W. 1979, private communication.
Rosner, R., and Vaiana, G. S. 1980, in *X-Ray Astronomy*, ed. R. Giacconi and G. Setti (Dordrecht: Reidel) p. 129.
Savage, B. D., Bohlin, R. C., Drake, J. F., and Budich, W. 1977, *Ap. J.*, **216**, 291.
Steward, F. D., Forman, W. R., Giacconi, R., Griffith, R. C., Harnden, F. R., Jones, C., and Pye, J. P. 1979, *Ap. J.*, **234**, L51.
Snow, T. P., Cash, W., and Grady, C. A. 1981, *Ap. J.* (*Letters*), **244**, L19.
Waldron, W. L. 1980, Ph.D. thesis, University of Wisconsin-Madison.

J. P. CASSINELLI and W. L. WALDRON: Washburn Observatory, University of Wisconsin-Madison, Madison, WI 53706

F. R. HARNDEN, JR., R. ROSNER, and G. S. VAIANA: Harvard-Smithsonian Center for Astrophysics, 60 Garden Street, Cambridge, MA 02138

W. T. SANDERS: Department of Physics, University of Wisconsin-Madison, Madison, WI 53706